MODELLING THE INITIATION AND EVOLUTION OF DAMAGE WITHIN GFRP BY INCLUDING REAL GEOMETRIC VARIABILITY

J.M. Gan, S. Bickerton*, M. Battley
Centre for Advanced Composite Materials, The University of Auckland, New Zealand
* Corresponding author: Dr. Simon Bickerton (s.bickerton@auckland.ac.nz)

Keywords: Textile Composites, Damage Initiation, Strength, Variability

1. Introduction

Textile composites have inherently high scatter in mechanical properties [1,2], requiring relatively high safety factors to be applied in structural design. Significant research has been conducted into the prediction of stiffness, strength, and the onset and evolution of damage [3,4]. Such work however, has been based upon idealised reinforcement geometries, and relatively little emphasis has been placed on the influence of variations within the reinforcement architecture. If the influence of such variations can be included into existing predictive methodologies, their influence can be assessed, and design procedures can be improved.

This paper presents a methodology for the introduction of the real geometric variability of glass-fibre reinforcements into existing damage modelling procedures. Real reinforcement structures are captured and modelled using a novel light transmission technique. Finite element (FE) models representing actual gauge regions of tensile specimens are generated and numerically tested within ABAQUS. A parallel experimental plan has been conducted to verify the damage predictions obtained.

2. Background

2.1. 3D textile modelling

3D textile modelling is commonly employed to investigate complex reinforcements that cannot be studied using simplified methodologies such as classical laminate theory. Common software tools used to generate 3D textile models include TexGen and WiseTex, both of which have been used to predict various mechanical and process properties [5,6]. 3D textile modeling allows incorporation of reinforcement architecture variations into property predictions [6], however little work has been presented incorporating *real* measured variations on a scale larger than a unit-cell.

2.2 Damage modelling

Prediction of damage initiation and evolution within loaded composite samples has been extensively covered in the literature. Continuous damage modelling (CDM) is a common approach used to simulate the effect of damage on a meso-scale. It is assumed that failed elements can be replaced by fictitious elements that have degraded elastic properties. The amount and method by which the properties are degraded differs between authors [4,7,8]. The main limitation of CDM approaches is that geometric damage such as crack propagation and distribution cannot be modeled [9], resulting in poor predictions of the final failure stress and strain.

3. Experimental methodology

To verify damage modelling predictions, a set of tensile specimens have been manufactured and tested. As a simplification, single layer samples have been used to eliminate the influence of non-uniform spatial nesting.

3.1. Sample preparation

Two E-glass fibre reinforcement structures were used for this study; an 800 g/m^2 plain weave (EWR) and an 825 g/m^2 bi-directional stitched (EB). A single layer 450×290 mm panel of each reinforcement type was manufactured with an epoxy resin (SP Prime20) using a modified resin infusion process, which utilised two glass mould surfaces to minimise the influence of surface finish and thickness variations on the results. Average thicknesses were 0.698 mm and 0.705 mm for the EWR and EB manufactured samples respectively. A diamond tipped cutting saw was employed to section each panel into 14 tensile specimen samples.

3.2. Physical testing

Tensile specimen testing was carried out on an Instron 5567 universal testing machine, following ASTM D30309. Physical extensometers could not be used due to their relatively high weight,

therefore strain was measured at the gauge region of the samples using a non-contact optical system. Samples were loaded until catastrophic failure, and photos of the EWR samples were captured post-failure to compare the damage regions to the developed model predictions. EB post-failure sample photos were not recorded, therefore the failure locations could not be compared.

4. Modelling methodology

The accumulation and evolution of damage during tensile loading of a single layer sample has been modeled to include real geometric variations, and is presented in this section. ABAQUS v6.10 and Intel Fortran Compiler 11.1 were employed.

4.1. Generation of real textile models

A novel method is used to obtain real geometric information describing the reinforcement architecture [10]. Prior to manufacturing of the panels, backlit photographs of light transmitted through dry reinforcement samples were captured, which were then processed within the MATLAB programming environment. The collected geometric information is read into the textile modeling software TexGen via a custom Python script, and the textile model generated. Fig. 1 presents example images of the EWR and EB reinforcements that have been converted into 3D textile models.

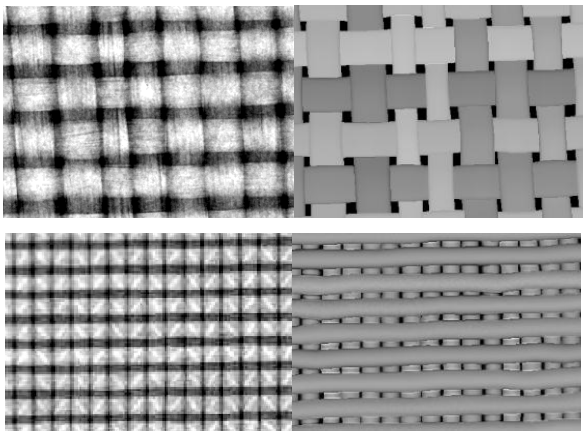

Fig. 1. (left) Real light transmission images and (right) TexGen generated reinforcement models of the EWR and EB fabrics

Models were created to represent the full gauge region of the tensile specimen, corresponding to roughly 50 and 128 unit cells of EWR and EB respectively. The gauge region was convenient as a direct strain measurement for this region was obtained using the optical strain measurement system. The experimental gauge regions have been defined within TexGen, and output as an ABAQUS input file (.inp) which contained the relevant mesh information. For the preliminary study presented here, a relatively coarse mesh refinement was employed to limit computational times, allowing a large number of simulations to be performed quickly. Voxel sizes were 0.8×0.8×0.11 mm and 0.47×0.61×0.097 mm (x,y,z) for the EWR and EB reinforcements respectively. This forced the tow cross-sections to be discrete. A mesh refinement study indicated that further refinement influenced only the ultimate failure, which is in agreement with work conducted in [4]. The influence of using such a coarse mesh is assessed later in this paper.

4.2. ABAQUS modeling

The standard ABAQUS output module of TexGen creates a FE mesh of C3D8R elements (8 node solid elements with reduced integration and hourglass control), providing only geometric and orientation information. A custom MATLAB script was written to modify the generated input file to include material properties for each element, and to assign boundary conditions for the model.

Table 1. Constituent material properties

Constituent property	Value
Isotropic epoxy resin properties	
E	3.2 GPa
v	0.35
G	1.2 GPa
Tensile strength	70 MPa
Compressive strength	70 MPa
Transversely isotropic E-glass properties	
E_L	53.0 GPa
E_T	24.4 GPa
v_{LT}	0.31
v_{TT}	0.3
G_{LT}	8.0 GPa
G_{TT}	4.6 GPa
Long. tens. strength	2000 MPa
Long. comp. strength	1000 MPa
Trans. tens. strength	80 MPa
Trans. comp. strength	250 MPa
Shear strength	100 MPa

Elements within the model were assumed to represent either pure matrix, or regions within the impregnated yarns. Matrix elements were modeled as isotropic, and impregnated yarn elements were modeled as transversely isotropic relative to the yarn orientation of the element. Using a packing

factor of 70 %, longitudinal and transverse yarn element properties were calculated using the rule-of-mixtures and Halpin-Tsai methods respectively. Failure strengths were defined based on various sources in the literature [4,11]. The resulting properties used for the ABAQUS simulations are presented in Table 1.

By modeling the entire gauge region, the applied boundary conditions are simplified when compared to traditional unit-cell models. It is assumed that the load conditions applied to the full size tensile specimen can also be applied to the gauge region. Fig. 2 presents a schematic detailing the boundary conditions applied to the textile models. The left set of nodes are fixed from moving in the load direction (x). The bottom and front set of nodes are fixed from moving in the y and z directions respectively to prevent rigid body motion. A constant velocity (v_x) of 2 mm/min is applied to the right surface nodes to replicate the loading rate defined in ASTM D3039. A constant simulation time step of 0.3 s was chosen, to provide practical solution times (<40 min).

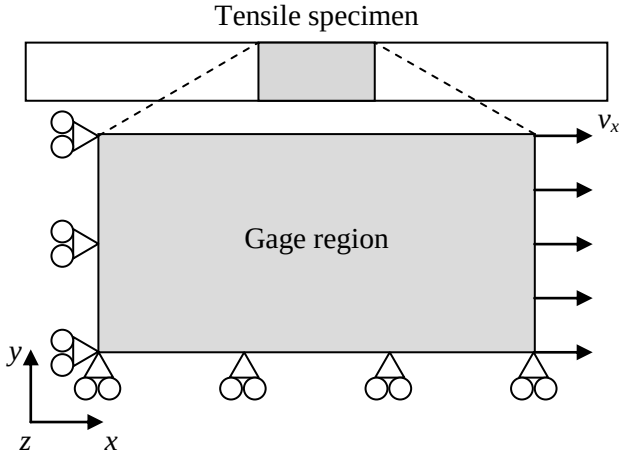

Fig 2. Schematic defining the applied boundary conditions to the gauge region ABAQUS models

4.3. Damage modeling

A continuous damage modeling (CDM) approach has been employed to simulate damage during loading. An ABAQUS UMAT material model subroutine has been written which is capable of modifying the elastic properties of elements during a simulation. Failure for both the resin and yarn elements is governed by the maximum stress criteria, which allows ABAQUS to determine the orientation of yarn failure (longitudinal or transverse) and degrade the elastic properties accordingly. As mentioned in literature [4,12], yarn element failure is orientation dependent (ie. the longitudinal tensile stiffness of yarns is relatively unaffected by transverse failure), therefore a set of selective degradation factors have been formed based on those presented in [4] to degrade element properties individually, which are shown in Table 2. Cumulative damage modes (ie. yarn failing initially in transverse tension, then failing in longitudinal tension) are taken into account by using the lowest degradation factor of the failure modes.

Table 2. Selective degradation factors

Failure mode	Degradation factors			
	E_L	E_T	G_{LT}	G_{LL}
Resin element selective degradation factors				
Max stress failure	0.05	0.05	0.05	0.05
Yarn element selective degradation factors				
Long. tension	0.002	0.05	0.05	0.05
Long. compression	0.002	0.05	0.05	0.05
Trans. tension	1.00	0.05	0.20	0.20
Trans. compression	1.00	0.05	0.20	0.20
Long. shear, LT-plane	1.00	0.05	0.05	1.00
Trans. shear, TT-plane	1.00	0.05	0.05	0.05

5. Results

FE models were created for each of the 14 EWR and EB experimental tensile specimen samples. Results obtained from the simulations are presented in the following sections.

5.1. Stress-strain data

Plots of the stress-strain data indicate the global response of a loaded tensile specimen (or gauge length for the FE model) and can be used to demonstrate the evolution and accumulation of damage during loading. Fig. 3 and 4 present the spread of EWR and EB loading curves respectivley. For clarity, only the maximum, minimum and middle-range experimental curves are shown.

Stress-strain data predicted using ABAQUS shows excellent correlation to the experiments. The experimental results are within the predicted spectrum of simulation results and the initial stiffness and progressive damage is captured well. This provides confidence in the developed modelling methodology, and indicates that the discretisation of the tow cross-section plays little role in the loading curve prior to ultimate failure. The statistical spread of the predicted EWR curves

is greater than the EB results. The applied reinforcement geometry is the only difference between models, indicating that the geometric variability is higher in the EWR samples. This is in agreement with previous work by the authors, which showed that tow dimension variability was generally lower in EB samples, as stitching reduces the ability for the tows to move in-plane [10].

Table 3. Comparison of statistical data for ultimate failure

	EWR samples		EB samples	
	Exp.	Model	Exp.	Model
σ (MPa)	350.3	314.2	377.2	498.3
COV	*5.0 %*	*9.5 %*	*6.2 %*	*6.2 %*
ε	0.026	0.021	0.022	0.029
COV	*8.6 %*	*7.5 %*	*6.4 %*	*5.7 %*

Table 3 compares statistical data for ultimate failure, based on each of the samples manufactured and tested. The simulation does not predict the final failure event very well, overpredicting and underpredicting ultimate stresses for the EB and EWR samples respectively. Errors in the prediction of final failure are expected due to sensitivity to mesh refinement. Further, poor final failure predictions is a recognised issue when using CDM techniques, as they cannot account for the distribution and propagation of crack-like defects [9]. Nevertheless, the presented simulations do provide a good indication to the level of variability (COV) that can be expected in experiment.

Table 4. Damage initiation points from the FE model

	EWR	EB
	Model	Model
σ_{ini} (MPa)	131.0	152.4
COV	*6.4 %*	*4.5 %*
ε_{ini}	0.0074	0.0068
COV	*8.1 %*	*5.8 %*

The initiation of damage typically occurs much earlier during application of load, relative to ultimate failure. Damage initiation strains, usually evident in the stress-strain curve as a knee or reduction in slope, are increasingly being considered as design criterion by structural engineers. The onset of damage can be easily identified in the results of CDM FE analyses, but can be difficult to determine from the experimental stress-strain curves alone. This is because load is predominantly transferred through the longitudinal tows [12], hence initial failure occurring within the resin plays little role in the overall response of the sample. Careful experiments are therefore required to determine onset of failure, using techniques such as acoustic emission (AE) or progressive sectioning and microscopic visual assesment. Such techniques are yet to be employed in this study, but will be used for comparison to the FE models presented here. Nevertheless, damage initiation values determined from the ABAQUS models are presented in Table 4.

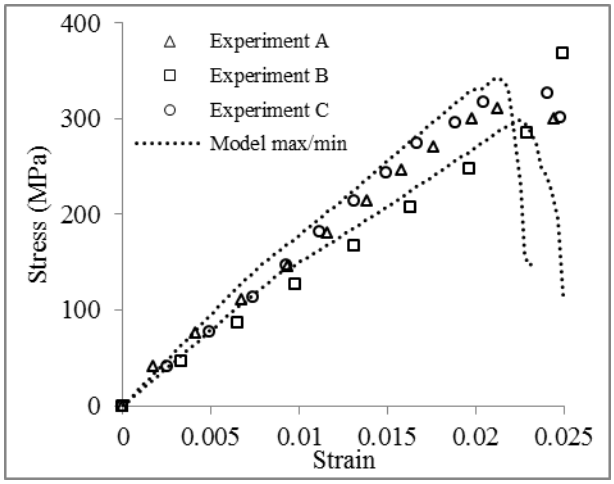

Fig. 3. Experimental and numerical stress-strain data for EWR samples

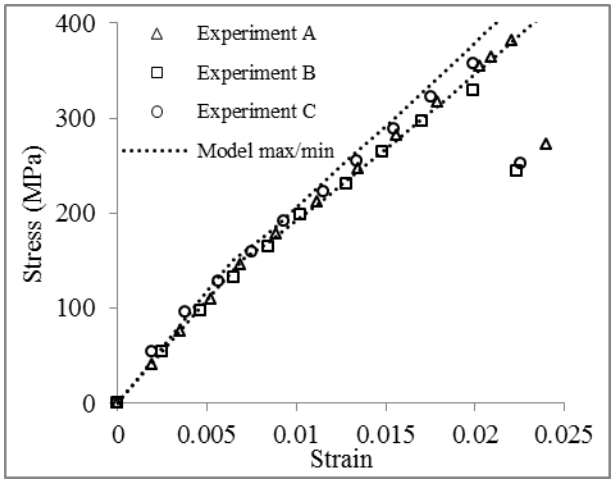

Fig. 4. Experimental and numerical stress-strain date for EB samples

5.2. Damage location

By incorporating geometric reinforcement variability into damage prediction methodologies, the regions in which damage initiates, and ultimate failure occurs, can be predicted. Fig. 5 presents an example ABAQUS EWR model solution, highlighting the regions where damage first begins, and how it evolves during loading. Fig. 5(a)-(d) show only the resin elements as the yarn elements are yet to fail, while Fig. 5(e)-(f) show both the resin and yarn elements separately. Green, red and blue elements represent undamaged, tensile failure and compressive failure respectively. Damage evolution begins with failure of the resin elements between the transverse tows (Fig. 5(b)), corresponding to a reduction in the stress-strain slope at the initiation point. This is followed by the failure of other remaining resin elements (Fig. 5(d)), until the longitudinal tows reach their maximum load, causing catastrophic failure (Fig. 5(f)). During experiments similar progression was observed, the transverse tows were seen to crack (but not fail) early during loading, but this was not registered as a reduction in stiffness in the loading curve. Such intra-tow cracking is undesirable for an in-service part. However, it is not possible to account for intra-tow cracking within a CDM approach, due to the homogenization of the tows that is conducted. Since this initial mode of failure plays little role in the overall response of the sample, the approach will not be modified in order to capture this effect.

Post-catastrophic failure meshes have been generated from the ABAQUS models, highlighting regions in which ultimate failure has initiated. Since the FE models represent the gauge region of a tensile specimen, only samples that fail within this region can be used for comparison. Fig. 6 shows four different EWR FE models (resin elements are hidden) and the corresponding experimental samples. Green and red elements represent undamaged, and tensile failure respectively. The presented FE models provide the capability to predict the location where catastrophic failure has occurred. While the results are for single layer samples only, good correlation between predicted and actual failure locations provides further confidence in both the geometric models (assumed square tow shape) and the developed damage methodology.

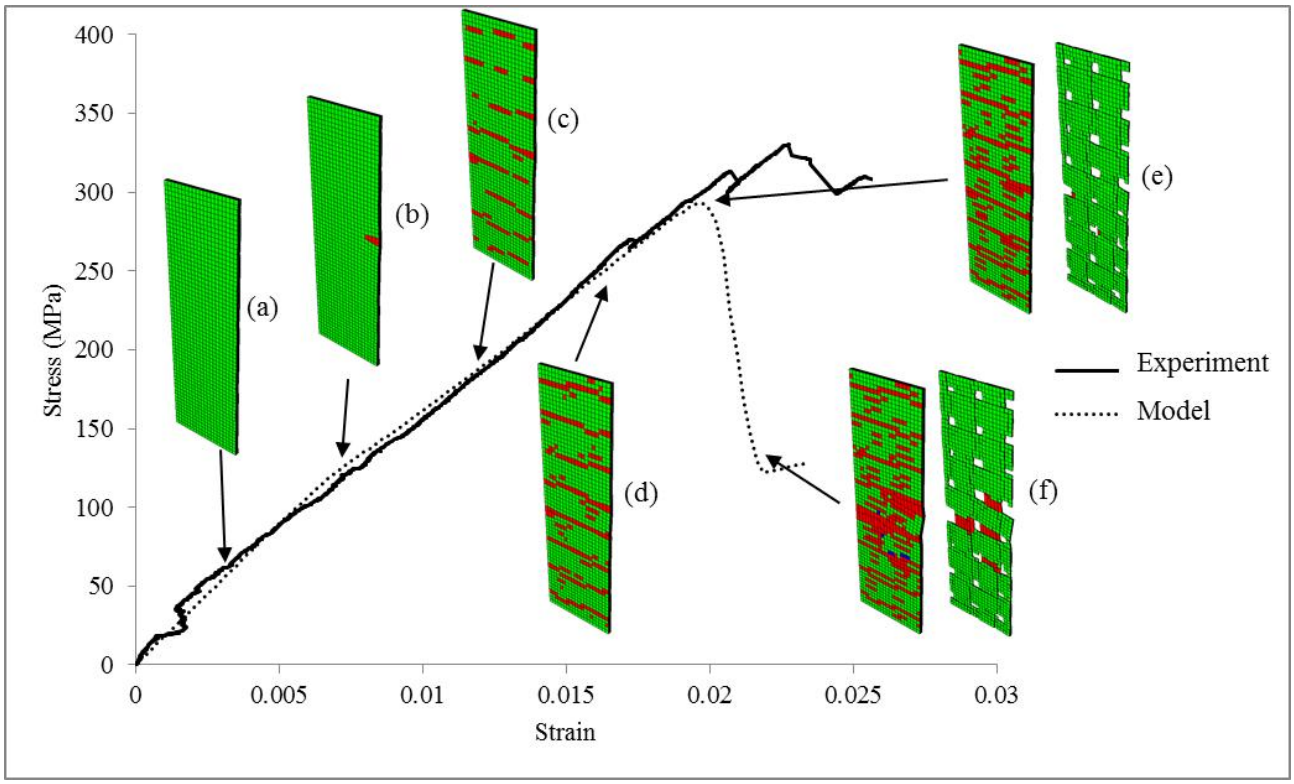

Fig. 5. Damage progression of the ABAQUS FE model during loading

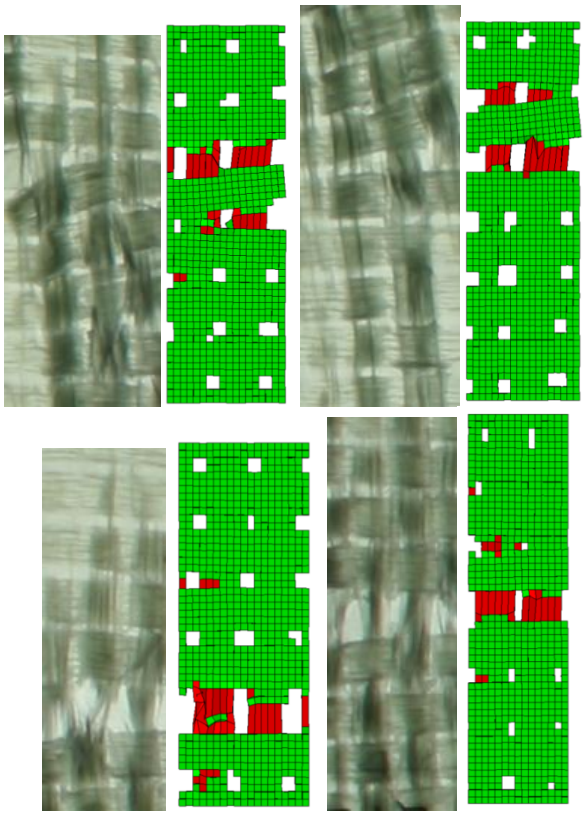

Fig. 6. Experimental and ABAQUS model EWR samples, post final failure

6. Conclusions

A methodology has been presented that is capable of including real geometric variability when predicting the initiation and evolution of damage caused by tensile loading within single layer glass fibre laminates. The damage initiation strain has been predicted for the manufactured samples, but has not yet been compared or verified with experiments. Good agreement was observed between the predicted and actual stress-strain curves, however the final failure event was poorly predicted. The location where catastrophic failure occurs has also been predicted, and correlates well to experiment.

7. Acknowledgements

This research is supported by the Ministry for Science and Innovation, and the University of Auckland.

The authors wish to acknowledge the contribution and support of Michael Bond, Dr. Louise Brown and Prof. Andrew Long from the University of Nottingham, UK.

8. References

[1] Berube KA, Lopez-Anido RA. "Variability of marine composite properties in a manufacturing round robin study" *Proceedings of 52nd International SAMPE Symposium*, Long Beach, CA, May 20-22, 2008

[2] Wang YJ, Li J. "Properties of composites reinforced with E-glass nonwoven fabrics" *Journal of Advanced Materials*, Vol. 26, Issue 3, pp 28-34, 1994

[3] Byström J, Jekabsons N, Varna J "An evaluation of different models for predication of elastic properties of woven composites" *Composites Part B: Engineering*, Vol. 31, Issue 1, pp 7-20, 2000

[4] Zhao LG, Warrior NA, Long AC "Finite element modelling of damage progression in non-crimp fabric reinforced composites" *Composites Science and Technology*, Vol. 66, Issue 1, pp 36-50, 2006

[5] Wong CC, Long AC, Sherburn M, Robitaille F, Harrison P, Rudd CD "Comparisons of novel and efficient approaches for permeability prediction based on the fabric architecture" *Composites Part A: Applied Science and Manufacturing*, Vol. 37, Issue 6, pp 847-857, 2006

[6] Desplentere F, Lomov SV, Woerdeman DL, Verpoest I, Wevers M, Bogdanovich AE "Micro-CT characterization of variability in 3D textile architecture" *Composites Science and Technology*, Vol. 65, Issue 13, pp 1920-1930, 2005

[7] Crookston J, Ruijter W, Long AC, Jones IA "Modelling mechanical performance including damage development for textile composites using a grid-based finite element method with adaptive mesh refinement" *Proceedings of the 8th International Conference on Textile Composites*, Nottingham, UK, Oct 16-18, 2006

[8] Turon A, Costa J, Maimi P, Trias D, Mayugo JA "A progressive damage model for unidirectional fibre-reinforced composites based on fibre fragmentation. Part I: Formulation" *Composites Science and Technology*, Vol. 65, Issue 13, pp 2039-2048, 2005

[9] Gorbatikh L, Ivanov D, Lomov SV, Verpoest I "On modelling of damage evolution in textile composites on meso-level via property degradation approach" *Composites Part A: Applied Science and Manufacturing*, Vol. 38, Issue 12, pp 2433-2442, 2007

[10] Gan JM, Bickerton S, Battley M "Automated characterization of variability in glass fibre reinforcement architecture" *Proceedings of the 10th International Conference on Textile Composites*, Lille, France, Oct 26-28

[11] Zenkert D "An introduction to sandwich composites" EMAS, 1995.

[12] Matzenmiller A, Lubliner J, Taylor RL "A constitutive model for anisotropic damage in fiber-composites" *Mechanics of Materials*, Vol. 20, pp 125-152, 1995